Desalination and Water Treatment
www.deswater.com

doi: 10.1080/19443994.2013.827779

52 (2014) 6784–6791
October

Taylor & Francis
Taylor & Francis Group

Oxidation of the insecticide dimethoate by Fenton and solar photo-Fenton processes using a lab-scale continuous flow reactor

Mabrouk Ben Brahim, Ridha Abdelhédi, Youssef Samet*

U.R. Electrochimie et Environnement, Département de Génie des matériaux, Ecole Nationale d'Ingénieurs de Sfax,
Université de Sfax, Route de Soukra, km 3.5, Sfax, B.P. 1173, 3038, Tunisia
Tel. +216 98660766; Fax: +216 74274437; email: sametyoussef @yahoo.fr

Received 31 August 2012; Accepted 26 June 2013

ABSTRACT

In this study, advanced oxidation processes utilizing Fenton's and solar photo-Fenton's reactions were investigated for the degradation of dimethoate, an organophosphorus insecticide extensively applied in agriculture. Effect of Fe^{2+}, H_2O_2, pH, and temperature on the degradation of this insecticide was studied. The kinetic rate constants (k_{app}) for COD removal were determined. The test results show that the degradation of dimethoate proceeded rapidly at pH value of 3.0. k_{app} enhanced with the increase of initial Fe^{2+} concentration and H_2O_2 dosing rate. However, higher levels of Fe^{2+} and H_2O_2 also inhibited the reaction kinetics. k_{app} decreased with the increase of initial dimethoate concentration, but increased with the increase of temperature. The activation energy for COD removal by Fenton oxidation, derived from the empirical Arrhenius expression, is $21.38\,\mathrm{kJ\,mol^{-1}}$. A noticeable k_{app} increase (~50%) was obtained when using the solar photo-Fenton process, which means about 50% gain of H_2O_2.

Keywords: Dimethoate; Fenton; Oxidation; Solar; COD; Removal

1. Introduction

Exposure to chemical pesticides causes a range of human health problems. It is estimated that nearly 10,000 deaths occur annually due to the excessive use of synthetic pesticides worldwide, with about three-fourths of these occurring in developing countries [1–3]. These chemicals can enter the aquatic environment through runoff from treated fields, from spillage, or from accidental discharge during production, packaging, storage, and waste disposal.

Dimethoate (Fig. 1) is a kind of high-effective pesticide that is extensively applied in agriculture; however, its residues have a negative effect on the environment, even on the health of people because of its toxicity and stability [4]. Dimethoate is one of the most frequently detected pesticides in surface and grounds waters [4,5]. Therefore, the innovative technologies for effectively and completely decomposing all organic pollutants are imperatively required.

In recent years, advanced oxidation processes (AOPs) have been intensively investigated for the treatment of waters and wastewaters. Such processes are based on the generation of the highly reactive hydroxyl radicals ($HO^{\bullet}$), which oxidize the organic matter in solution and, in favorable cases, convert it completely into water, carbon dioxide, and inorganic compounds.

---

*Corresponding author.

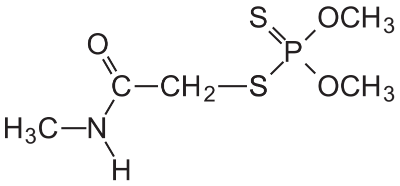

Fig. 1. Chemical structure of dimethoate.

The main reactions taking place between hydroxyl radicals and organic compounds in solution may involve hydrogen abstraction Eq. (1) [6–8], or hydroxyl addition Eq. (2) [7].

$$\mathrm{RH} + \mathrm{HO}^{\cdot} \rightarrow \mathrm{R}^{\cdot} + \mathrm{H_2O} \rightarrow \text{Products} \quad k_1 = 10^7 \ (\mathrm{L\ mol^{-1}\ s^{-1}}) \tag{1}$$

$$\mathrm{R} + \mathrm{HO}^{\cdot} \rightarrow \mathrm{HOR}^{\cdot} \rightarrow \text{Products} \quad k_2 = 10^7 \ (\mathrm{L\ mol^{-1}\ s^{-1}}) \tag{2}$$

$HO^{\bullet}$ are produced *in situ* by chemical [9,10], ultrasonic irradiation [11], electrochemical [12–14], and/or photochemical [15] reactions. In the Fenton process, this is attained by the reaction between H_2O_2 and ferrous ions:

$$\mathrm{Fe^{2+}} + \mathrm{H_2O} \rightarrow \mathrm{Fe^{3+}} + \mathrm{HO}^{\cdot} + \mathrm{OH^-} \quad k_3 = 63 \ (\mathrm{L\ mol^{-1}\ s^{-1}}) \tag{3}$$

The slow regeneration of Fe^{3+} to Fe^{2+} by hydrogen peroxide (Eq. (4)) is the rate-determining step of the overall reaction:

$$\mathrm{Fe^{3+}} + \mathrm{H_2O_2} \rightarrow \mathrm{Fe^{2+}} + \mathrm{HO_2^{\cdot}} + \mathrm{H^+} \quad k_4 = 0.01 \ (\mathrm{L\ mol^{-1}\ s^{-1}}) \tag{4}$$

In the photo-Fenton process, however, the rate of Fe^{2+} regeneration is significantly increased by the interaction of light and complexes in solution, producing additional hydroxyl radicals, as represented by Eq. (5):

$$\mathrm{Fe^{3+}} + \mathrm{H_2O_2} + hv \rightarrow \mathrm{HO}^{\cdot} + \mathrm{Fe^{2+}} + \mathrm{H^+} \tag{5}$$

In recent years, a number of papers have appeared in the literature describing the application of the photo-Fenton process to the photodegradation of aqueous solutions containing different organic compounds [16–18]. The main disadvantage of the photo-Fenton process, represented by the energy consumption by electrical UV lamps, can be overcome by using sunlight [19–21].

The degradation of dimethoate was studied using different processes. The sonolytic degradation of aqueous solutions of dimethoate was examined by Yao et al. [22]. Optimal degradation rates were obtained at 619 kHz for continuous sonolysis and 406 kHz for pulse sonolysis. The primary pathways for degradation include hydroxyl radical oxidation, hydrolysis, and pyrolysis on collapsing cavitation bubble interfaces. More than 90% toxicity of dimethoate was reduced within 45 min ultrasonic irradiation.

Evgenidou et al. [23] studied the photocatalytic degradation of dimethoate using the photo-assisted Fenton reaction under different conditions. The UV irradiation experiments were carried out in a 500 mL Pyrex UV reactor equipped with a diving Philips HPK 125 W high-pressure mercury lamp. This system achieved high degradation rates. Three by-products were identified (O,O-dimethyl phosphonic ester, O,O,S-trimethylphosphorothioate, and omethoate or dimethoxon (O,O-dimethyl-S-methylcarbamoylmethyl phosphorothioate)). Chen et al. [24] investigated the photocatalytic mineralization of dimethoate in aqueous solutions using nanosized TiO_2 powder at different conditions. Four possible by-products such as omethoate were identified by means of GC–MS.

Previous solar photo-Fenton degradation of dimethoate has been performed [25]. The pH was adjusted to 2.7–2.9 with sulfuric acid in order to avoid iron hydroxide precipitation. The total dose of hydrogen peroxide was always added at the beginning after pH adjustment. However, the effect of several experimental parameters such as initial concentration of dimethoate, iron, and H_2O_2 doses, temperature, and pH were not investigated.

In addition, no research has been focused specifically in solar photo-Fenton degradation of this pesticide using a continuous addition of H_2O_2 in the reactor. So that this work evaluates the degradation of dimethoate by solar photo-Fenton process at different experimental parameters including H_2O_2 dosing rate, initial concentrations of dimethoate and Fe^{2+}, temperature, and pH. Benefits of solar radiations on the oxidation reaction efficiency were also exhibited.

2. Experimental

2.1. Reagents

All solutions were prepared in the laboratory. These solutions contain quantities of dimethoate taken from an emulsifiable concentrate (Biomat 40 EC from Arysta Lifescience) containing 400 g L^{-1} dimethoate.

All the solutions were freshly prepared with double distilled water. Ferrous sulfate heptahydrate ($FeSO_4$ $7H_2O$) was obtained from Riedel-de Haën (Seelze-Hannover, Germany) and used as the Fe(II) catalyst. Hydrogen peroxide (35% v/v) and sulfuric acid were provided by Merck (Darmstadt, Germany).

2.2. Experimental design and methodology

The experiments were done in an experimental device, whose scheme is shown in (Fig. 2). The installation consists of: (1) an Erlenmeyer flask at which the pesticide solution was prepared. This Erlenmeyer flask was immersed in water bath to control the working temperature by a thermostat (Julabo Labortechnik GMBH, Sellback, Germany). The treated volume was 1 L; the solution was circulated through the reactor using a peristaltic pump (Cole-Parmer Instrument, Chicago, Illinois 60648 USA) with a flow rate of $140\,\mathrm{mL\,min^{-1}}$. This pump is simultaneously used to introduce H_2O_2 solution in the Erlenmeyer flask at a flow rate of $0.7\,\mathrm{mL\,min^{-1}}$. The quantity of the ferrous sulfate was introduced into the solution at startup. The pH values were adjusted using a prepared 1 M sulfuric acid solution and measured using a pH meter (PHM multi-parameter analyzer, pH/mV Belgium Kingdom). The solutions were continuously stirred using a magnetic stirrer (Tacussel, France). (2) Solar reactor; this prototype was designed based on a compound parabolic collector. The reactor consists of a borosilicate glass tube (4.5 m length, an inner diameter of 6 mm, and outer diameter of 8 mm) snake-shaped placed 34 degrees to the horizontal.

The solar photo-Fenton experiments were performed at the National Engineering School of Sfax (approximately 3 m above sea level, latitude: 34° 44′ N, longitude: 10° 45′ E), Tunisia. All tests were conducted between 11:00 a.m. and 3:00 p.m. on the sunny days from April to June 2010. The global solar radiation intensity was approximately $850\,\mathrm{W/m^2}$.

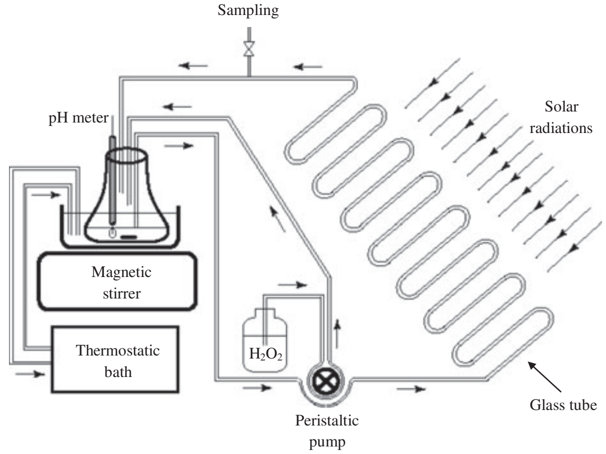

Fig. 2. Scheme of the experimental installation.

For tests using dark Fenton reagent, the experimental device was kept away from solar radiation by covering with a black plastic film and an aluminum foil.

2.3. Analysis

Samples (0.5 mL) were withdrawn from the reactor at selected intervals for COD analysis. COD was measured using a spectrophotometer (*Shimadzu UV*-Mini 1240 UV/Vis Spectrophotometer) using a dichromate solution as the oxidant in strong acid media [26].

Since the residual H_2O_2 interferes with the measurement of COD [27], the residual amount of H_2O_2 was also measured using the permanganate titration. This method is suitable for measuring solutions of hydrogen peroxide in the range 0.25–70% wt [28]. Correction of hydrogen peroxide interference was performed to COD analysis.

3. Results and discussion

3.1. Oxidation of dimethoate by Fenton process

3.1.1. Effect of the initial concentration of ferrous ion

To evaluate the effect of ferrous ion, the experiments were conducted on various amounts of ferrous ion as shown in Fig. 3. Initial conditions were $930\,\mathrm{mg\,L^{-1}}$ COD_0, $40\,\mathrm{mg\,min^{-1}}$ hydrogen peroxide dosing rate, temperature 25°C, and pH 3.0. In all tests,

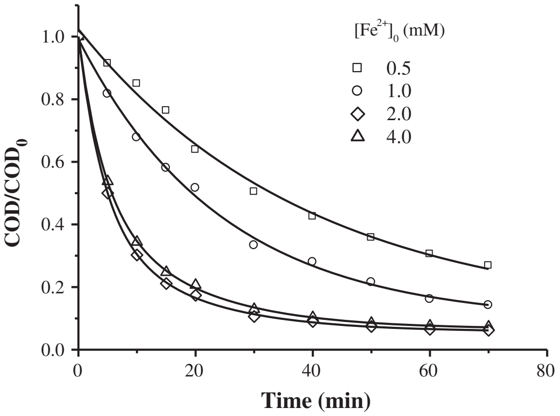

Fig. 3. Effect of initial Fe^{2+} concentration on the COD removal by Fenton process. The inset panel shows k_{app} evolution at different Fe^{2+} concentrations. $COD_0 = 930\,\mathrm{mg\,L^{-1}}$; H_2O_2 dosing rate $= 40\,\mathrm{mg\,min^{-1}}$; pH = 3.0; and $T = 25$°C.

Table 1
Kinetic degradation of dimethoate by Fenton process

$[Fe^{2+}]_0$ (mM)		0.5	1.0	2.0	3.0	4.0
Pseudo-first-order	R^2	0.9623	0.9544	0.9642	0.9472	0.9472
Pseudo-second-order	R^2	0.9956	0.9874	0.9967	0.9966	0.9975
$k_{app} \times 10$ ($L\,g^{-1}\,min^{-1}$)		0.391	0.842	2.676	2.455	0.225

the drop in COD was more significant during the first minutes of reaction where the concentration of organic matter is high. This observation is clearly observed in the case of 2 mM ferrous ion. The data taken from Fig. 3 clearly indicate that the pseudo-second-order model gives better prediction rather than the pseudo-first-order for COD removal as indicated by the higher regression coefficients (R^2) values (Table 1). It is worth noting that several authors reported that the decaying profile of COD obtained by Fenton oxidation of organic molecules can follow pseudo-second-order kinetics [29,30].

If we suppose that the hydroxyl radical concentration is constant during treatment, the COD removal rate r can be given by the following equation:

$$r = -\frac{\mathrm{dCOD}}{\mathrm{d}t} = k[\mathrm{HO}^{\cdot}]^{\alpha}\mathrm{COD}^2 = k_{\mathrm{app}}\mathrm{COD}^2 \qquad (6)$$

α is the reaction order related to the hydroxyl radicals, k is the real rate constant, and k_{app} is the global apparent rate constant for COD removal.

Integration of this equation subject to the initial condition $COD = COD_0$ at $t = 0$ leads to the following equation:

$$1/\mathrm{COD} - 1/\mathrm{COD}_0 = k_{\mathrm{app}}\, t \qquad (7)$$

In this case, a plot of $1/COD—1/COD_0$ vs. time in every experiment must lead to a straight line whose slopes are k_{app} values. For example, Fig. 4 shows this plot related to Fig. 3.

It can be seen from Fig. 5 that increasing the Fe^{2+} concentration from 0.5 to 2 mM enhanced k_{app} values. It results in the multiplication of the k_{app} by factors of 7 when $[Fe^{2+}]_0$ increases from 0.5 to 2 mM. So, the highest removal efficiency of COD was achieved when Fe^{2+} concentration of 2 mM was applied.

It was known that Fe^{2+} had a catalytic decomposition effect on H_2O_2. When Fe^{2+} concentration increased, the catalytic effect also accordingly increased. However, for Fe^{2+} doses higher than 2.0 mM, the k_{app} values decreased slightly. This decrease is essentially due to competitive consumption of $HO^{\bullet}$ radicals (Eq. (8)).

$$\mathrm{Fe}^{2+} + \mathrm{HO}^{\cdot} \rightarrow \mathrm{Fe}^{3+} + \mathrm{OH}^- \qquad (8)$$

It is worth noting that, in the Fenton process, the amounts of Fe^{2+} ions should be as low as possible for economic and environmental reasons; high amounts of Fe^{2+} ions might produce a larger quantity of Fe^{3+} sludge. The removal/treatment of the

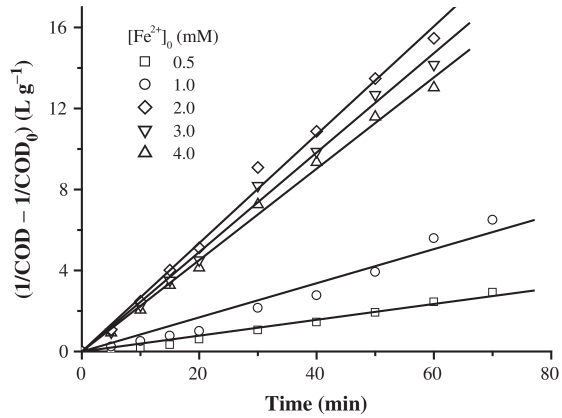

Fig. 4. Plot of $(1/COD-1/COD_0)-t$ at different initial Fe^{2+} concentration. $COD_0 = 930\,mg\,L^{-1}$; H_2O_2 dosing rate = $40\,mg\,min^{-1}$; pH = 3.0; and $T = 25°C$.

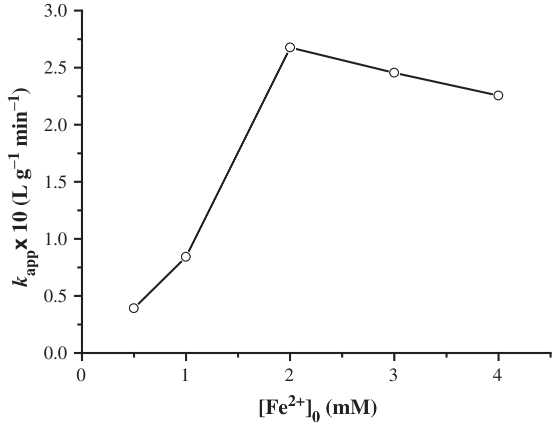

Fig. 5. k_{app} evolution at different initial Fe^{2+} concentration. $COD_0 = 930\,mg\,L^{-1}$; H_2O_2 dosing rate = $40\,mg\,min^{-1}$; pH = 3.0; and $T = 25°C$.

sludge-containing Fe^{3+} at the end of the wastewater treatment is expensive and needs large amount of chemicals and manpower [31].

3.1.2. Effect of hydrogen peroxide dosing rate

The dosing rate of H_2O_2 is considered as one of the most important factor which should be considered in the Fenton process. The effect of the dosing rate of hydrogen peroxide on the efficiency of the oxidation process was investigated under the operating conditions ($COD_0 = 930\,mg\,L^{-1}$, $[Fe^{2+}]_0 = 2\,mM$, pH = 3.0, and $T = 25^\circ C$) (Fig. 6). It was found that COD removal efficiency increases with increasing the dosing rate of hydrogen peroxide from 10 to $50\,mg\,min^{-1}$ and decreased for higher dosing rate of H_2O_2. Excessive H_2O_2 reacts with $HO^\bullet$ (Eq. (9)) competing with organic pollutants and consequently reducing treatment efficiency.

$$H_2O_2 + HO^\cdot \rightarrow HO_2^\cdot + H_2O \tag{9}$$

Moreover, the inset of Fig. 6 shows the variation of the apparent rate constants values, at different H_2O_2 dosing rate calculated from the straight lines considering a pseudo-second-order reaction. k_{app} increased significantly when the dosing rate of H_2O_2 increased until $50\,mg\,min^{-1}$, due to the effect of the additional produced $HO^\bullet$ radicals, but for H_2O_2 dosing rate higher than $50\,mg\,min^{-1}$, k_{app} decreased. Hence, $50\,mg\,min^{-1}$ H_2O_2 appears as an optimal dosing rate.

3.1.3. Effect of the initial dimethoate concentration

The effect of dimethoate concentration on the degradation efficiency was investigated at different initial concentrations (COD_0: 564, 930, and $1,289\,mg\,L^{-1}$) and presented in Fig. 7. It can be observed that the COD removal decreased with the increase of the initial concentration of the pollutant. Almost 90% of COD removal was achieved after about 50 min time of reaction for COD_0 564 and $930\,mg\,L^{-1}$. Higher time did not improve the COD percent removal. However, at high dimethoate concentration, the removal of COD needs more time and so more quantity of H_2O_2 (e.g. the percent removal of COD is about 75% after 70 min when using $COD_0 = 1,289\,mg\,L^{-1}$). This is because when the concentration of dimethoate increases, the quantity of hydroxyl radicals produced continuously with time does not increase accordingly and hence the removal rate decreases. Also, from the inset of Fig. 7, it can be seen that k_{app} decreased with COD_0. This behavior was similar to those reported by many researchers [32–34].

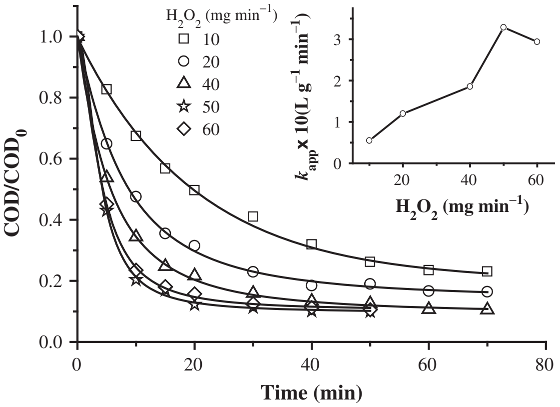

Fig. 6. Effect of H_2O_2 dosing rate on the trend of COD/COD_0 ratio during the oxidation of chlorpyrifos solution by Fenton process. $[Fe^{2+}]_0 = 2.0\,mM$; $COD_0 = 930\,mg\,L^{-1}$, pH = 3.0; and $T = 25^\circ C$.

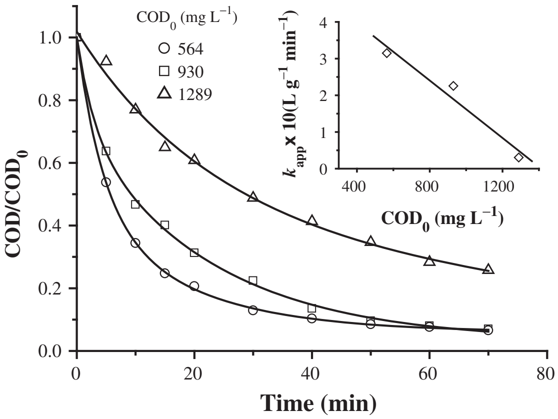

Fig. 7. Effect of initial chlorpyrifos concentration on the COD removal by the Fenton process. The inset panel shows k_{app} evolution at different initial COD. H_2O_2 dosing rate = $40\,mg\,min^{-1}$; $[Fe^{2+}]_0 = 2.0\,mM$; pH = 3.0; and $T = 25^\circ C$.

3.1.4. Effect of the initial pH

It is well known that the optimum pH in Fenton reaction is between 2.5 and 4.0 [35]. In this work, the effect of initial pH of pesticide solution on the degradation of dimethoate by Fenton process was carried out in the pH range between 2.5 and 4.0. The results are shown in Fig. 8. It is found that COD removal rate is maximum at pH 3.0. This is also elucidated by k_{app} values. Indeed, below pH 2.5, three mechanisms will decrease the efficiency of the reaction: (i) ferrous complex formation; (ii) inhibition of the reaction between Fe^{2+} and H_2O_2 [36]; and (iii) enhancement of hydroxyl radical scavenging by H^+ at low pH [33].

k_{app} decreased at pH values higher than 3.0, because ferric ions precipitate as iron hydroxide

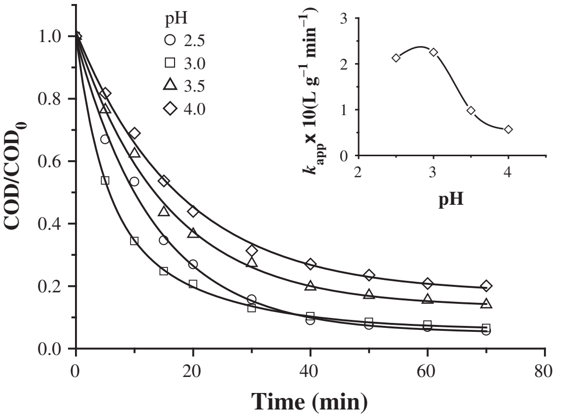

Fig. 8. Effect of initial pH on the COD removal by the Fenton process. The inset panel shows k_{app} evolution at different pH. H_2O_2 dosing rate = 40 mg min^{-1}; $[Fe^{2+}]_0$ = 2.0 mM; COD_0 = 930 mg L^{-1}; and T = 25 °C.

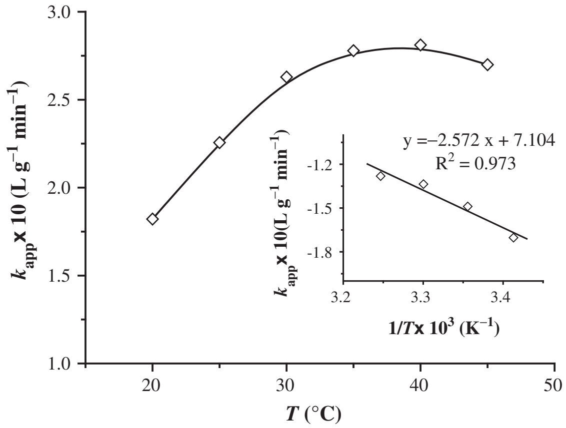

Fig. 9. Evolution of k_{app} at different temperatures. The inset shows the plot of Ln k_{app}–(1/T). COD_0 = 930 mg L^{-1}; H_2O_2 dosing rate = 40 mg min^{-1}; $[Fe^{2+}]_0$ = 2.0 mM; and pH = 3.0.

$Fe(OH)_3$. This precipitate is very stable ($K_s = 10^{-38}$), the reduction of Fe^{3+} in Fe^{2+} is very slow, and the regeneration of Fe^{2+}, as an initiator of $HO^{\bullet}$ radical production, becomes the rate-limiting step of the process. Moreover, at pH above 3.0, the concentration of hydroperoxyl anions (HO_2^- conjugate base of H_2O_2) increases. The hydroperoxyl anions formed reduced the concentration of H_2O_2 and $HO^{\bullet}$ radical (Eqs. (10) and (11)).

$$H_2O_2 + HO_2^- \rightarrow H_2O + O_2 + HO^- \tag{10}$$

$$HO^{\bullet} + HO_2^- \rightarrow H_2O + O_2^{\bullet}- \tag{11}$$

3.1.5. *Effect of the temperature*

It is well known that an increase in the temperature of a reaction medium leads to an acceleration in the rate of the reaction. The effect of temperature on the oxidative degradation of dimethoate was assessed by running Fenton reaction within a temperature range of 20–45 °C at pH 3.0, H_2O_2 dosing rate 40 mg min^{-1}, $[Fe^{2+}]_0$ 2.0 mM, and COD_0 930 mg L^{-1}. The results are shown in Fig. 9. It was found that k_{app} is significantly affected by reaction temperature and increased with the raising of temperature with an optimal value of 40 °C. The decrease of k_{app} at temperature higher than 40 °C is due to the accelerated decomposition of H_2O_2 into oxygen and water as it has been reported by [37].

The temperature dependence of the kinetic parameters of Fenton treatment was calculated by Eq. (12). [38]. The Gibbs free energy (ΔG), the enthalpy (ΔH), and the entropy (ΔS) for the Fenton process were also obtained using Eqs. (13) and (14).

$$\ln k_{app} = \ln A - (E_a/RT) \tag{12}$$

$$\Delta G = -RT \ln k_{app} \tag{13}$$

$$\ln k_{app} = (\Delta S/R) - (\Delta H/RT) \tag{14}$$

where k_{app} is the global apparent rate constant for COD removal, A is the Arrhenius constant, E_a is the activation energy, R is the ideal gas constant (8.314 J mol^{-1} K^{-1}), and T is the reaction absolute temperature.

Due to the narrow temperature range employed in this study (i.e. 20–40 °C), variations of the Arrhenius constant and the activation energy of the empirical Arrhenius expressions of the COD removal may be neglected. The variation of lnk_{app} vs. $1/T$ is plotted in the inset of Fig. 9. Good linear relationships exist between the plot of lnk_{app} and $1/T$ (regression coefficient was higher than 0.97). The results of the thermodynamic calculations are shown in Table 2.

The negative value for the Gibbs free energy showed that the Fenton process was spontaneous in nature and that the degree of spontaneity of the reaction decreased by increasing temperature.

3.2. *Oxidation of dimethoate by solar photo-Fenton process*

In order to improve the reaction rate and COD abatement efficiency, solutions were subjected to solar radiation. Fig. 10 shows the trend of the COD/COD_0

Table 2
Thermodynamic parameters for COD removal by Fenton process

T (K)	$\ln k_{app}$	ΔG (kJ mol^{-1})	ΔH (kJ mol^{-1})	ΔS (J mol^{-1} K^{-1})	E_a (kJ mol^{-1})
293	−1.703	−4.141	21.38	59.06	21.38
298	−1.489	−3.683			
303	−1.336	−3.360			
308	−1.280	−3.272			
313	−1.269	−3.297			

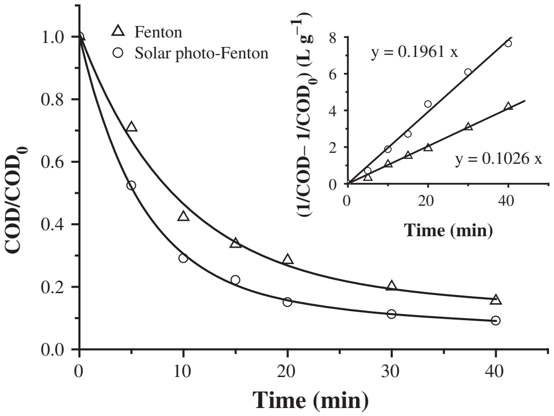

Fig. 10. Trend of COD/COD$_0$ ratio during the oxidation of chlorpyrifos solution by Fenton and solar phto-Fenton reactions. The inset panel shows the fitting of the experimental data to a second-order reaction kinetic model for the two processes. H_2O_2 dosing rate = 50 mg min^{-1}; $[Fe^{2+}]_0$ = 2.0 mM; COD$_0$ = 1,300 mg L^{-1}; pH = 3.0; and T = 40°C.

ratio during the treatment of dimethoate solution by the two processes under the optimum experimental conditions already found when using Fenton process (H_2O_2 = 50 mg min^{-1}, $[Fe^{2+}]_0$ = 2.0 mM, pH = 3.0, and T = 40°C). It can be seen that the solar photo-Fenton system needed less time and consequently less quantity of H_2O_2 to reach the same COD recent removal. In fact, under the optimum experimental conditions, the solar photo-Fenton process need a dose of H_2O_2 50% lower than that used in the Fenton process to remove 85% of COD. The inset of Fig. 10 shows that k_{app} in solar photo-Fenton process is almost twice as high as in Fenton process.

The results obtained with this preliminary study suggest that solar photo-Fenton is a promising pretreatment process for pesticides wastewater.

4. Conclusion

In this study, the results showed that dark Fenton and solar photo-Fenton processes are powerful methods for the degradation of the insecticide dimethoate, but the solar photo-Fenton process is 50% more efficient than Fenton process. The degradation rate by the two processes can be expressed as a pseudo-second-order reaction with respect to COD. COD removal was influenced by the dosing rate of the hydrogen peroxide, the initial concentration of dimethoate, the amount of iron salt, the pH of solution, and the temperature. The optimum conditions were observed at pH 3, with an initial Fe^{2+} concentration of 2.0 mM and H_2O_2 dosing rate of 50 mg min^{-1}. The experiments carried out at the temperature range 20–45°C showed an optimum COD removal at 40°C and allowed computation of the apparent activation energy (21.38 kJ mol^{-1}).

Acknowledgment

This research is funded by the Tunisian Higher Education and Scientific Research Ministry.

References

[1] L. Horrigan, R.S. Lawrence, P. Walker, How sustainable agriculture can address the environmental and human heath harms of industrial agriculture, Environ. Health Perspect. 110 (2002) 445–456.
[2] D. Fatta, C. Michael, St. Canna-Michaelidou, M. Christodoulidou, Pesticides, volatile and semivolatile organic compounds in the inland surface waters of Cyprus, Desalination 215 (2007) 223–236.
[3] J.H. Yen, K.H. Lin, Y.S. Wang, Potential of the insecticides acephate and methamidophos to contaminate groundwater, Ecotoxicol. Environ. Saf. 45 (2000) 79–86.
[4] N. Dujaković, S. Grujića, M. Radišića, T. Vasiljevića, M. Laušević, Determination of pesticides in surface and ground waters by liquid chromatography–electrospray–tandem mass spectrometry, Anal. Chim. Acta 678 (2010) 63–72.
[5] M.H. El-Saeid, A.M. Al-Turki, M.I. Al-Wable, G. Abdel-Nasser, Evaluation of pesticide residues in Saudi Arabia ground water, Res. J. Environ. Sci. 5 (2011) 171–178.
[6] Y.W. Kang, K.Y. Hwang, Effects of reaction conditions on the oxidation efficiency in the Fenton process, Water Res. 34 (2000) 2786–2790.
[7] V. Flotron, C. Delteil, Y. Padellec, V. Camel, Removal of sorbed polycyclic aromatic hydrocarbons from soil, sludge and sediment samples using the Fenton's reagent process, Chemosphere 59 (2005) 1427–1437.
[8] J.H. Sun, S.P. Sun, M.H. Fan, H.Q. Guo, L.P. Qiao, R.X. Sun, A kinetic study on the degradation of p-nitroaniline by Fenton oxidation process, J. Hazard. Mater. 148 (2007) 172–177.
[9] R. Andreozzi, V. Caprio, A. Insola, R. Marotta, Advanced oxidation processes (AOP) for water purification and recovery, Catal. Today 53 (1999) 51–59.
[10] Y. Samet, M. Ayadi, R. Abdelhédi, Degradation of 4-chloroguaiacol by dark Fenton and solar photo-Fenton advanced oxidation processes, Water Environ. Res. 81 (2009) 2389–2397.
[11] J.J. Yao, N.Y. Gao, C. Li, L. Li, B. Xu, Mechanism and kinetics of parathion degradation under ultrasonic irradiation, J. Hazard. Mater. 175 (2010) 138–145.
[12] E. Hmani, S. Chaabane Elaoud, Y. Samet, R. Abdelhédi, Electrochemical degradation of waters containing o-Toluidine on PbO_2 and BDD anodes, J. Hazard. Mater. 170 (2009) 928–933.

[13] Y. Samet, L. Agengui, R. Abdelhédi, Electrochemical degradation of chlorpyrifos pesticide in aqueous solutions by anodic oxidation at boron-doped diamond electrodes, Chem. Eng. J. 161 (2010) 167–172.

[14] Y. Samet, L. Agengui, R. Abdelhédi, Anodic oxidation of chlorpyrifos in aqueous solution at lead dioxide electrodes, J. Electroanal. Chem. 650 (2010) 152–158.

[15] M.T.A. Silva, E. Nouli, N.P. Xekoukoulotakis, D. Mantzavinos, Effect of key operating parameters on phenols degradation during H_2O_2 assisted TiO_2 photocatalytic treatment of simulated and actual olive mill wastewaters, Appl. Catal. B 73 (2007) 11–22.

[16] J. Arana, E.T. Rendón, J.M.D. Rodríguez, J.A.H. Melián, O.G. Díaz, J.P. Pena, Highly concentrated phenolic wastewater treatment by the photo-Fenton reaction, mechanism study by FTIR-ATR, Chemosphere 44 (2001) 1017–1023.

[17] D. Kassinos, M. Constantinou, N. Varnava, A. Papadopoulos, S. Vlachos, D. Mantzavinos, Oxidation of pesticides in water by Fenton and photo-Fenton reactions, J. Adv. Oxid. Technol. 11 (2008) 246–253.

[18] M.M. Martin Ballesteros, J.A. Sanchez Perez, J.L. Casas Lopez, I. Oller, S. Malato Roddriguez, Degradation of a four-pesticide mixture by combined photo-Fenton and biological oxidation, Water Res. 43 (2009) 653–660.

[19] D. Robert, A. Piscopo, J.V. Weber, Selective solar photodegradation of organo-pollutant mixtures in water, Sol. Energy 77 (2004) 553–558.

[20] J.M. Monteagudo, A. Durán, I. San Martín, M. Aguirre, Effect of continuous addition of H2O2 and air injection on ferrioxalate-assisted solar photo-Fenton degradation of Orange II, Appl. Catal. B 89 (2009) 510–518.

[21] Y. Samet, I. Wali, R. Abdelhédi, Kinetic degradation of the pollutant guaiacol by dark Fenton and solar photo-Fenton processes, Environ. Sci. Pollut. Res. 18 (2011) 1497–1507, doi: 0.1007/s11356-011-0514-4.

[22] J.J. Yao, M.R. Hoffmann, N.Y. Gao, Z. Zhang, L. Li, Sonolytic degradation of dimethoate: Kinetics, mechanisms and toxic intermediates controlling, Water Res. 45 (2011) 5886–5894.

[23] E. Evgenidou, I. Konstantinou, K. Fytianos, I. Poulios, Oxidation of two organophosphorous insecticides by the photo-assisted Fenton reaction, Water Res. 41 (2007) 2015–2027.

[24] J.Q. Chen, Z.J. Hu, D. Wang, C.J. Gao, R. Ji, Photocatalytic mineralization of dimethoate in aqueous solutions using TiO_2: Parameters and by-products analysis, Desalination 258 (2010) 28–33.

[25] I. Oller, W. Gernjak, M.I. Maldonado, P. Fernandez-Ibanez, J. Blanco, J.A. Sanchez-Perez, S. Malato, Degradation of the insecticide dimethoate by solar photocatalysis at pilot plant scale, Environ. Chem. Lett. 3 (2005) 118–121.

[26] I.M. Kolthof, E.B. Sandell, E.J. Meeehan, S. Buckstein, Quantitative Chemical Analysis, 4th ed., Macmillan, New York, 1969, pp. 1862–1867.

[27] N. Kang, D.S. Lee, J. Yoon, Kinetic modeling of Fenton oxidation of phenol and monochlorophenols, Chemosphere 47 (2002) 915–924.

[28] S.H. Lin, C.C. Lo, Fenton process for treatment desizing wastewater, Water Res. 31 (1997) 2050–2056.

[29] A.M.F.M. Guedes, L.M.P. Madeira, R.A.R. Boaventura, C.A.V. Costa, Fenton oxidation of cork cooking wastewater – overall kinetic analysis, Water Res. 37 (2003) 3061–3069.

[30] C. Ratanatamskul, P. Auesuntrachun, Removal of COD and colour from old-landfill leachate by advanced oxidation processes, Int. J. Environ. Waste Manage. 4 (2009) 470–480.

[31] J.H. Ramirez, C.A. Costa, L.M. Madeira, G. Mata, M.A. Vicente, M.L. Rojas-Cervantes, A.J. Lopez-Peinado, R.M. Martin-Aranda, Fenton-like oxidation of Orange II solutions using heterogeneous catalysts based on saponite clay, Appl. Catal. B 71 (2007) 44–56.

[32] M. Tamimi, S. Qourzal, N. Barka, A. Assabbane, Y. Ait-Ichou, Methomyl degradation in aqueous solutions by Fenton's reagent and the photo-Fenton system, Sep. Purif. Technol. 61 (2008) 103–108.

[33] M.S. Lucas, J.A. Peres, Decolorization of the azo dye reactive black 5 by Fenton and photo-Fenton oxidation, Dyes Pigm. 71 (2006) 236–244.

[34] N. Modirshahla, M.A. Behnajady, F. Ghanbary, Decolorization and mineralization of C.I. acid yellow 23 by Fenton and photo-Fenton processes, Dyes Pigm. 73 (2007) 305–310.

[35] H. Gallard, J. De Laat, B. Legube, Effect of pH on the oxidation rate of organic compounds by FeII/H_2O. Mechanisms and simulation, New J. Chem. 22 (1998) 263–268.

[36] J. Sanz, J.I. Lombrana, A.M. De Louis, M. Ortueta, F. Varona, Microwave and Fenton's reagent oxidation of wastewater, Environ. Chem. Lett. 1 (2003) 45–50.

[37] S. Wang, A comparative study of Fenton and Fenton-like reaction kinetics in decolorisation of wastewater, Dyes Pigm. 76 (2008) 714–720.

[38] Y.S. Ho, J.C.Y. Ng, G. McKay, Kinetics of pollutant sorption by biosorbents: Review, Sep. Purif. Methods 29 (2000) 189–232.